Romanian Journal of Petroleum & Gas Technology
VOL. VI (LXXVII) • No. 2/2025

EVALUATION OF THE GEOCHEMICAL AND PETROGRAPHIC CHARACTERISTICS OF THE INKISI FORMATION IN THE SEDIMENTARY BASIN OF THE CENTRAL BASIN

Jean Iyolo Lungembo [1*], Joël Etshekodi Lohadje [1,3], Serge Diemo [1,4], Dona Kampata Mbwelele [1], Adalbert Makutu Mangwayaya [2]

[1] Exploration-Production Department, Faculty of Oil, Gas and Renewable Energies, University of Kinshasa, D.R. Congo
[2] Geosciences Department, Faculty of Science, University of Kinshasa, D.R. Congo
[3] National Geological Service of Congo, D.R. Congo
[4] Centre National de Télédétection, D.R. Congo
* email (corresponding author): jean.iyolo@unikin.ac.cd

DOI: 10.51865/JPGT.2025.02.08

ABSTRACT

The Congo Craton, located in the central depression, hosts an interior sedimentary basin covering over 800,000 km², subdivided into four intracontinental sub-basins: Busira, Lokoro, Lomami, and Bushimayi. The formation of this vast Neoproterozoic basin results from an initial stretching of the lithospheric crust followed by thermal subsidence, corresponding to the rebalancing of the lithosphere during the Pan-African orogenic cycle. This tectonic activity led to the formation of pull-apart basins, reflecting the generalized subsidence of the craton in the central depression. The general lithostratigraphic column of the basin comprises five sedimentary sequences, among which the Inkisi sandstone formation is central to our study as a potential reservoir rock. The analysis of the deposits and sedimentary evolution of this formation is essential for determining its porosity and permeability, key characteristics for a hydrocarbon reservoir.

The choice of the southwestern part of the basin, specifically on the outskirts of the provincial city of Kinshasa, is motivated by the accessibility of this rock and the absence of in-depth studies in this area. This research aims to enhance the understanding of the geological characteristics of the Inkisi formation, particularly in a context that has never been studied in depth. Geochemical analysis and the assessment of the alteration state of the rocks will provide unprecedented information on their petrographic potential. By highlighting aspects such as porosity and permeability, this study offers new perspectives for oil exploration in the central depression.

Despite the importance of the Inkisi formation, previous research has often overlooked a detailed analysis of its petrographic and sedimentary characteristics. Few studies have been conducted on the southwestern portion of the basin, particularly regarding geochemical properties and the alteration state. This study aims to fill these gaps by providing a comprehensive and integrated analysis that could serve as a basis for future research and the exploitation of natural resources in the region.

Keywords: sedimentary basin, intracontinental sub-basins, Inkisi Formation, DR Congo, porosity, permeability.

INTRODUCTION

The interior sedimentary basin of the central depression covers an area of over 800,000 km². It is subdivided into four intracontinental sub-basins [25]. The establishment of this extensive Neoproterozoic basin resulted from an initial stretching of the lithospheric crust followed by thermal subsidence, corresponding to the rebalancing of the lithosphere during the Pan-African orogenic cycle [6],[7],[19]. These tectonics led to the formation of pull-apart basins arranged in four main faults named: the Busira sub-basin, the Lokoro sub-basin, the Lomami sub-basin, and the Bushimayi sub-basin, reflecting the generalized subsidence of the Congo craton in the central depression [26]. The general lithostratigraphic column of the central basin [5],[25], consists of five sedimentary sequences made up of several geological formations, among which the Inkisi sandstone formation is the focus of our study as a potential reservoir rock among others found in this basin [1],[2]. The study of the deposits and sedimentary evolution of this rock, considered a potential hydrocarbon reservoir in the basin's petroleum system, is of great importance for determining its porosity and permeability, which are key characteristics for a hydrocarbon reservoir rock [5],[19].

The choice of the southwestern part of the basin, specifically on the periphery of the provincial city of Kinshasa, is motivated by the accessibility of this rock and the fact that this area has never been the subject of an appropriate study [4],[23]. This research is of great importance as it contributes to a better understanding of the geological characteristics of the Inkisi formation, particularly in the context of a region that has never been thoroughly studied [5],[7]. The geochemical analysis and assessment of the alteration state of the rocks will provide unprecedented information about their petrographic potential [5],[19]. By highlighting aspects such as porosity and permeability, this study offers new perspectives for oil exploration in the central depression. [1],[3],[24].

Despite the importance of the Inkisi formation, previous research has often overlooked a detailed analysis of its petrographic and sedimentary characteristics [4],[6]. Few studies have been conducted on the southwestern portion of the basin, especially regarding geochemical properties and the state of alteration [1],[5]. This study aims to fill these gaps by providing a comprehensive and integrated analysis that could serve as a basis for future research and for the exploitation of natural resources in the region [18].

This study focuses on the geochemical and petrographic analysis of the Inkisi formation in the sedimentary basin of the central depression. It aims to determine the physical and chemical properties of this rock, such as porosity and permeability, which are essential for assessing its potential as a hydrocarbon reservoir [5],[7].

Although the Inkisi formation is of great geological importance, previous research has generally overlooked a thorough exploration of its petrographic and sedimentary characteristics, particularly in the southwestern region of the basin [1],[4]. This study aims to fill this gap by providing a detailed analysis of the geochemical properties and the state of alteration of the rocks, which have not been sufficiently examined to date [5],[19].

The novelty of this research lies in its integrated approach, combining geochemical, petrographic, and sedimentary analyses to provide a comprehensive view of the Inkisi formation. Furthermore, the results of this study will provide unprecedented information about the petrographic potential of this formation, thereby opening new perspectives for oil exploration in the central depression and contributing to a better understanding of the natural resources in the region [1],[10],[19].

MATERIALS AND METHODS

To achieve our objective we used:

a) Documentation:

- A bibliographic review of the local geology of the West Congolian Supergroup, based on various online documents.

b) In the field, during the geological survey, we used the following equipment:

- GPS, magnifying glass, geologist's hammer, marker, tape measure, compass, 10kg weight, and notebook.

c) In the laboratory, we will use a microscope for petrographic analysis, (Figure 1) and:

- Google Colab: this programming language for creating graphics.
- ArcGIS-10.8: This software enabled us to create maps related to the study area.

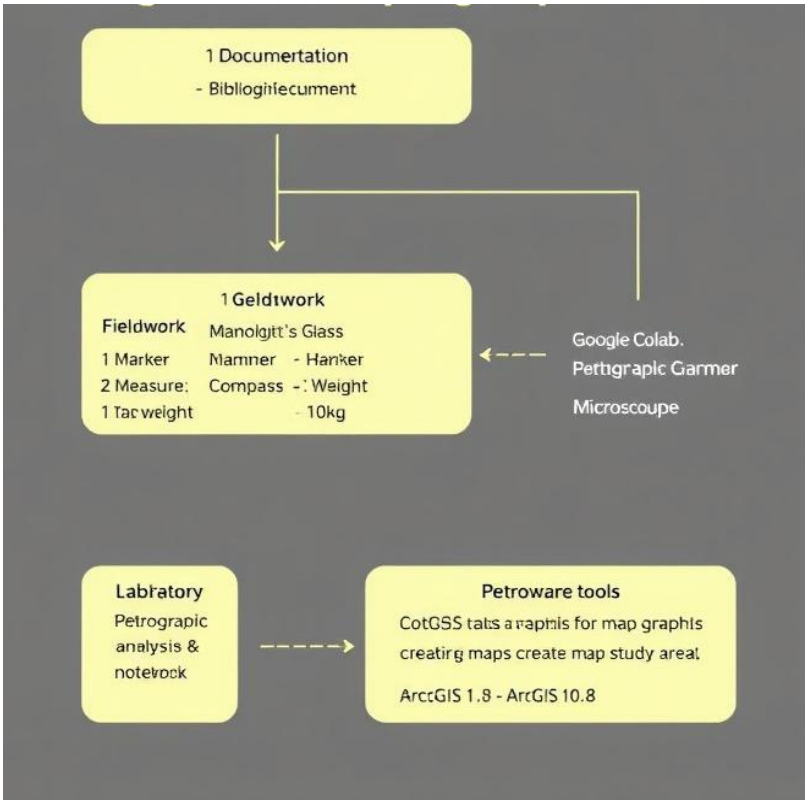

Figure 1. *Graphic summary of the article*

GEOGRAPHICAL CONTEXT

Located in the southwestern part of the city province of Kinshasa and Central Kongo, the artisanal sites of Kinsuka, the N'djili Brewery site, the Kimwenza site, the Kasangulu site, and the Zongo site (Figure 2) are located respectively at 04°22'0'' south latitude and 15°11'0.10'' east longitude, 04°27'23.7'' south latitude and 15°20'21.8'' east longitude, 04°28'46.4'' south latitude and 15°16'31.2'' east longitude, 04°34'53.874" south latitude and 15°11'56.97 east longitude, 04°46'14.202'' south latitude and 14°52'4.296'' east longitude [1],[4],[6],[9]. Field analytical data is recorded according to site order.

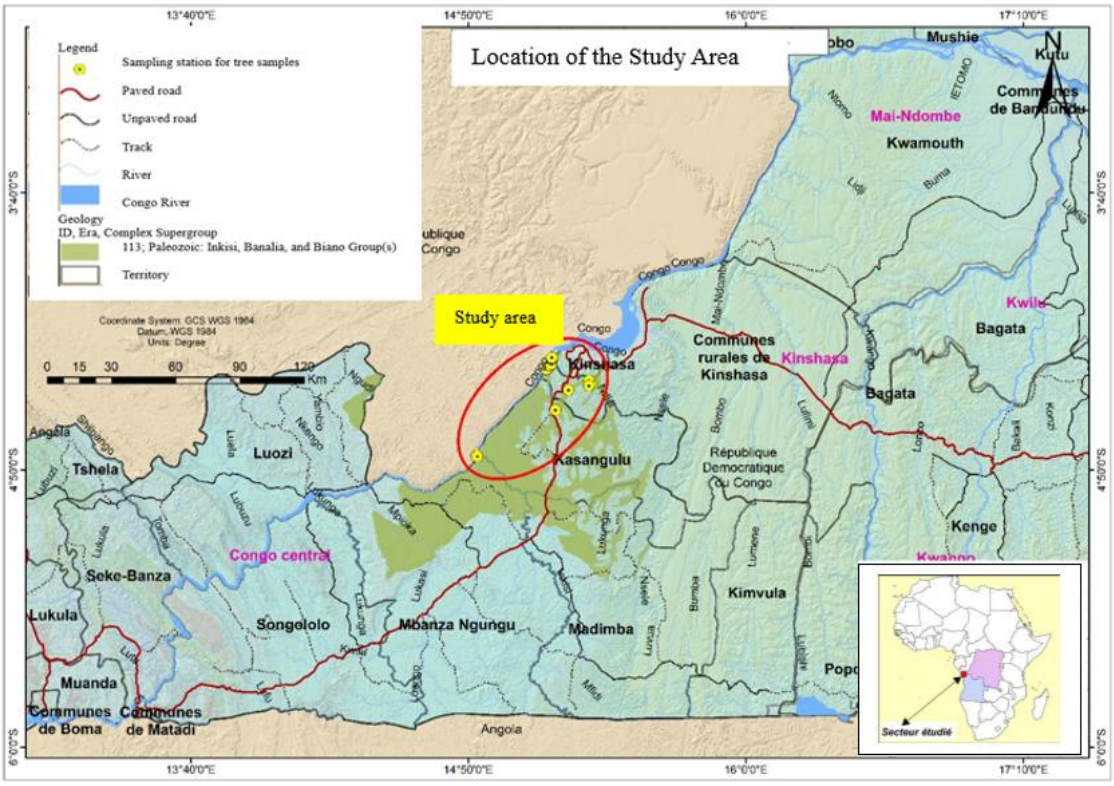

***Figure 2**. Map of the study area*

ON THE KINSUKA WEBSITE

As we head towards the waterfall, we observe pockets on the outcrop, suggesting dissolution, but in sandstone. Is there calcite present? We can clearly see the details of the bedding in the rock, as well as a conglomerate layer between two banks consisting of more or less rounded pebbles (Figure 3). The cliff is 120 m long. On a cliff not far from the site, we observe a sequence of sandstone benches containing calcite and a conglomerate layer with altered sandstone cement containing more or less rounded pebbles (Figure 4) [8],[27].

***Figure 3**. View of the NG station at ground level, Probable rock type: Sandstone*

***Figure 4**. View of the NG 2B station at ground level, Probable rock type: Sandstone*

Station 3 Ngudiabaka

Macroscopically, we observe coarse-grained microconglomeratic sandstone. The upper part is dark purple in color, while the lower part is light purple. In addition, there is a 5 cm thick layer of calcite between these two-colored areas (Figure 5).

***Figure 5**. View of the NG 3C station at ground level, Probable rock type: Sandstone*

Station 8 SFC

The outcrop has an average grain size and is characterized by a purple color. The rock is arranged in a massive bank, where some parts consist of medium to coarse pebbles, visible at the outcrop scale (Figure 6).

***Figure 6**. View of the SFC / KS station at ground level, Probable rock type: Sandstone*

N'DJILI BREWERY SITE

Station 12 ND

- **Macroscopic description**

The upper part of the benches is broken into slabs, while the lower part is solid. Purple in color, there is a purple-colored rock face, the upper part of which is weathered and the lower part of which is compact. Medium grain size with traces of calcite (Figure 7).

Figure 7. *View of the ND 1 station at ground level, Probable rock type: Sandstone*

KIMWENZA SITE

Station 2 KM

- **Macroscopic description**

Observations made on the working face at the Kimwenza site (ech 2) reveal the presence of sandstone rock with notable geological characteristics: The rock has a color ranging from mauve to greenish, with an average grain size. The black color on the rock is explained by the rise of groundwater. The formation appears in the form of banks of varying sizes. (ech 21) are mauve, greenish, and fine-grained (Figure 8) [5],[12].

Figure 8. *View of the outcrop at station KM 1, Probable rock type: Sandstone*

KASANGULU SITE

- **Macroscopic description**

The rock ranges in color from dark gray to light brown. It appears massive to slightly banded, with irregular surfaces and subhorizontal or subvertical planes of fracturing. Granules visible to the naked eye are likely present, suggesting a medium to coarse grain size. The formation shows poorly defined planes of stratification (Figure 9).

***Figure 9**. View of the KG station at ground level, Probable rock type: Sandstone*

ZONGO SITE

Station 1 Chinese quarry

- **Macroscopic description**

Purple coloration with some green traces of calcite. The rock consists of six thick layers with medium grain size. The layers run in a north-south direction. (Figure 10).

***Figure 10**. View of station ZG, Probable rock type: Sandstone*

PETROGRAPHIC AND GEOCHEMICAL ANALYSIS OF THE COLLECTED ROCK SAMPLES

Petrographic analysis

The petrographic analysis includes macroscopic and microscopic descriptions of rock samples taken from our study area [7],[8],[12]. The microscopic analysis includes six (6) thin sections. The minerals were identified under a polarizing microscope using the criteria established by [11],[21],[22].

❖ Sample NG - Microscopic description

Under the microscope, the rock exhibits a coherent structure. This is highlighted by white or gray quartz crystals and plagioclase crystals in poly-synthetic twins in Non-Analyzed Polarized Light (LPNA)and colorless twins in Analyzed Polarized Light (LPA). The quartz grains are fine, medium-sized, and coarse; they have subrounded, subangular, and angular shapes; the contours of these grains are partly smooth and partly jagged. The plagioclase grains are medium-sized; they lie between the quartz grains with a few iron oxide grains and iron oxide films and have subangular and elongated shapes (Figure 11).

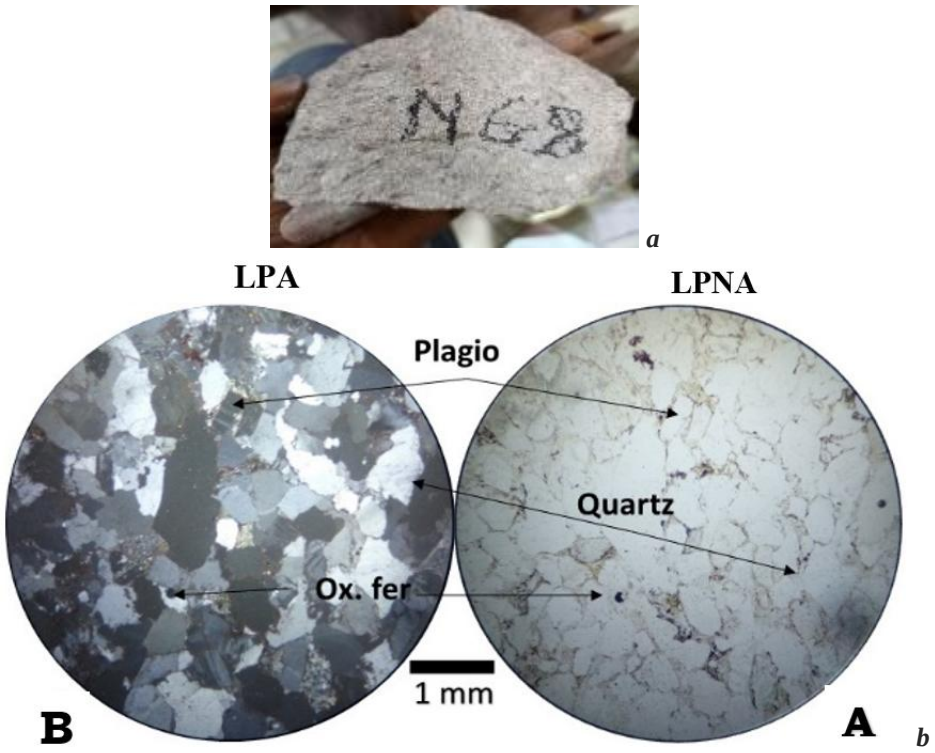

Figure 11*.a. Macroscopic view; b. Microscopic view of the sandstone. (Photo in the laboratory).*

❖ Sample KS (SFC) - Microscopic description

Under the microscope, the rock exhibits a coherent structure. This is highlighted by large white or gray (LPA) and colorless (LPNA) quartz grains, between which isolated plagioclase grains with poly-synthetic twins (LPA) and colorless (LPNA) grains can be observed. The quartz grains are fine, medium-sized, and coarse, and have rounded, subrounded, and subangular shapes. Most of the medium-sized and coarse grains are cracked (Figure 12).

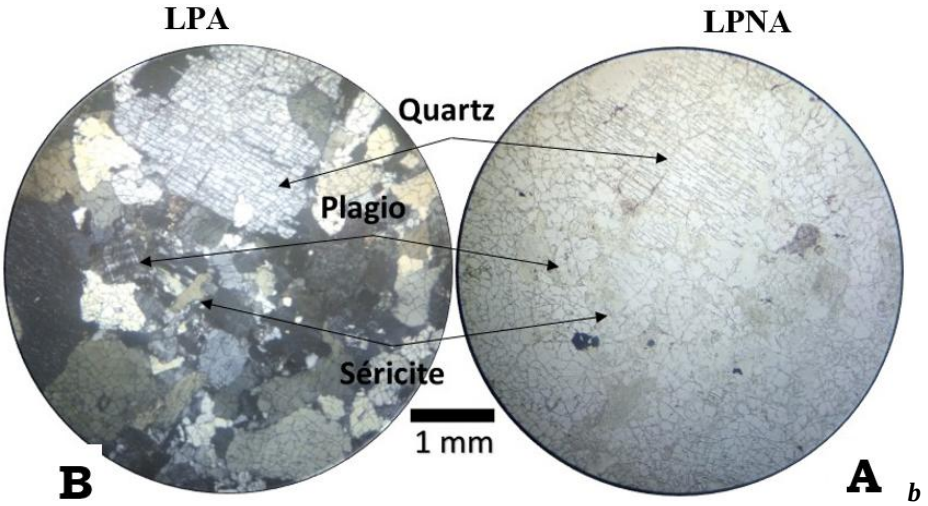

***Figure 12**.a. Macroscopic view; b. Microscopic view of the sandstone (Photo in the laboratory).*

❖ **Sample ND 1 - Microscopic description**

Under the microscope, the rock exhibits a coherent structure. This is highlighted by white or gray (LPA) and colorless (LPNA) quartz grains, as well as microcline grains with lattice twins (LPA) and colorless twins (LPNA). The quartz grains are subangular, angular, subrounded, and elongated. The microcline grains are subrounded. Between these grains are yellow (LPA) and green (LPNA) chlorite flakes. The arrangement of the chlorite flakes gives the rock a lineation. The rock also contains iron oxide accumulations (Figure 13).

a

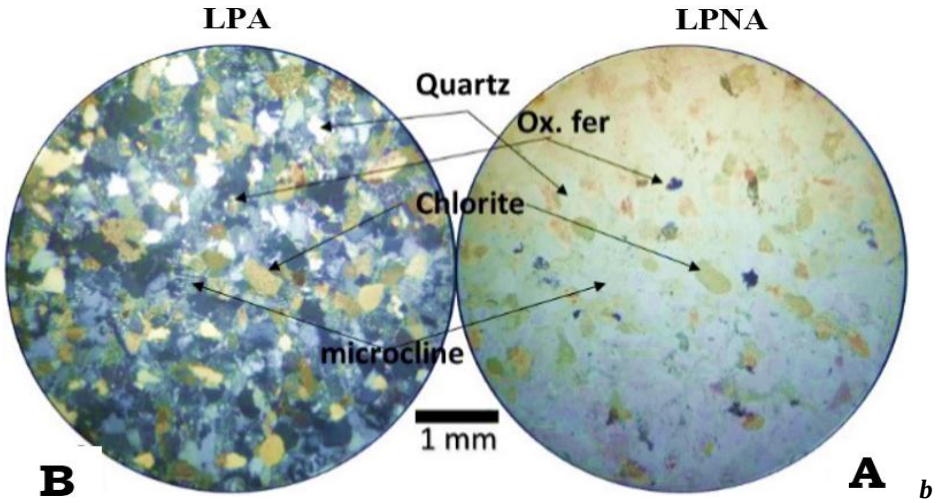

***Figure 13**.a. Macroscopic view; b. Microscopic view of sandstone (Photo in the laboratory)*

❖ Sample KM - Microscopic description

Under the microscope, the rock has a very dense texture. This is highlighted by white or gray (LPA) and colorless (LPNA) quartz grains, as well as plagioclase grains with polysynthetic twins (LPA) and colorless (LPNA) grains. The quartz grains are subangular, angular, subrounded, and elongated. The plagioclase grains are elongated. Between these grains are sericite flakes with a moiré-like appearance (LPA) and colorless sericite flakes (LPNA). The orientation of the quartz grains and sericite flakes gives the rock a lineation. The rock also contains iron oxide accumulations. The orientation of these accumulations gives the rock a lineation (Figure 14).

a

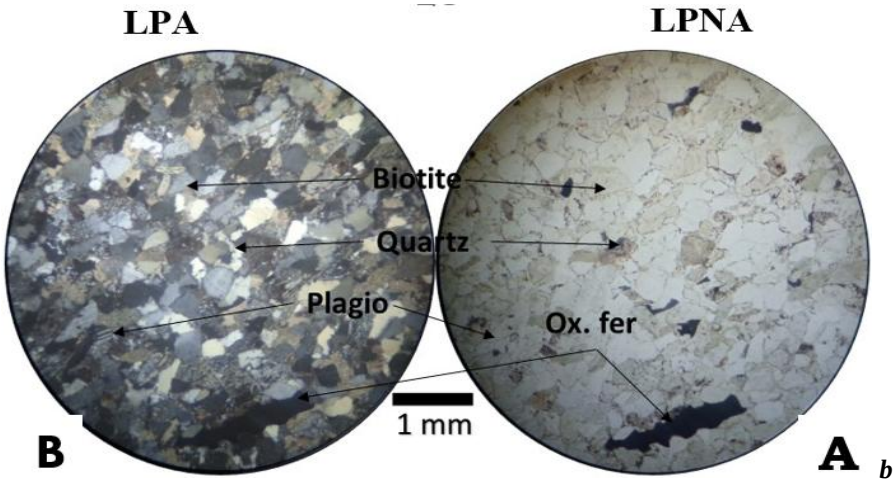

b

***Figure 14**.a. Macroscopic view; b. Microscopic view of sandstone (Photo in the laboratory).*

❖ Sample KG - Microscopic description

Under the microscope, the rock exhibits a matrix consisting mainly of quartz silt. This matrix comprises white or gray (LPA) and colorless (LPNA) quartz grains, as well as rare crystals of microcline with lattice twins (LPA) and colorless (LPNA). Between these crystals are moiré-like (LPA) and colorless (LPNA) sericite flakes, brown (LPA) and (LPNA) biotite flakes, and yellowish (LPA) and green (LPNA) chlorite flakes. The arrangement of these various flakes gives the rock a lineation; grains and accumulations of form oxide can also be observed (Figure 15).

a

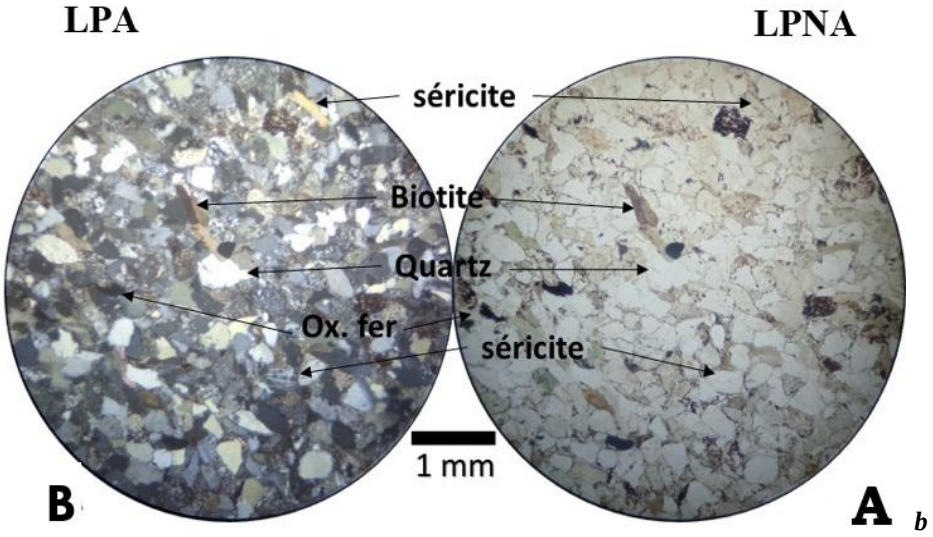

Figure 15*.a. Macroscopic view; b. Microscopic view of the sandstone (Photo in the laboratory).*

❖ **Sample ZG - Microscopic description**

Under the microscope, the rock has a jointed texture. This is highlighted by small grains of white or gray quartz (LPA) and colorless quartz (LPNA), interspersed with small flakes of sericite with a moiré appearance (LPA) and colorless sericite (LPNA). The quartz grains are fine to very fine; they are rounded, sub-rounded, sub-angular, angular, and elongated in shape (Figure 16).

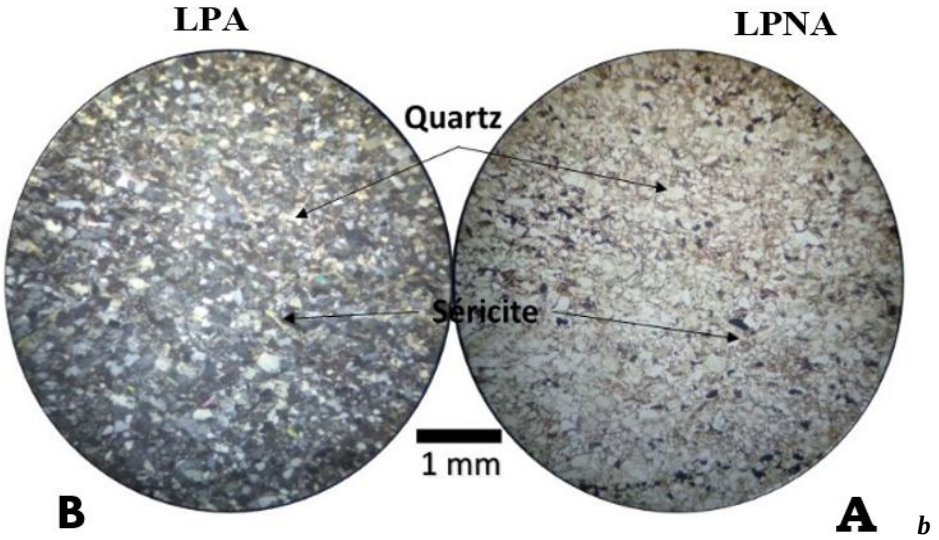

Figure 16.*a. Macroscopic view. b. Microscopic view of the sandstone (Photo in the laboratory).*

GEOCHEMICAL STUDIES

In this section of our work, we present the results of geochemical analyses of rock samples collected in the field. A total of six samples were subjected to these analyses, which were performed using energy dispersive X-ray fluorescence (XRF) spectrometry. These analyses were carried out at the CRENK central analysis laboratory using a XEPOS fluorescence spectrometer.

The procedure used to analyze the various samples can be summarized as follows:

- **Analytical Protocol and Calculation Method**

The elements (ions) were measured using the energy dispersive X-ray fluorescence spectrometer (ED-XRF), XEPOS III, using the "FP-Pellets CGEA" and "TQ-Pellets Fast" methods of the XEPOS III spectrometer. The powders "ISE PER 2012-1-2, a clay soil coded 863; ISE PER 2012-1-4, a sandy clay soil coded 962; ISE PER 2013-1-4, a clay soil coded 961, SOIL-7, and CRM GBW07408 containing certain elements of interest were used as standards [9]. The X-ray fluorescence spectrometer is a multi-element method using four secondary targets, namely molybdenum (39.76 kV voltage and 0.88 mA current), aluminum oxide (49.15 kV voltage and 0.7 mA current), cobalt (35.79 kV voltage and 1 mA current), and finally Bragg's HOPG Crystal (17.4 kV voltage and 1.99 mA current) from the palladium anode [16].

- **Principle**

In general, the sample (a pellet) to be analyzed is placed under an X-ray beam. Under the effect of the X-rays, the sample "resonates" and re-emits its own X-rays—this is fluorescence [17]. If we look at the energy spectrum of the fluorescent X-rays, we see peaks characteristic of the elements present, so we know which elements we have, and the height of the peaks allows us to determine their quantities.

- **Calculation method**

The normalized intensities of the spectrometer are proportional to the concentrations used to calculate the concentrations of our samples by external calibration [14]. The Kα1 peak (3.313 keV) of K was used for the calculation, and the Bragg HOPG Crystal target (17.4 kV voltage and 1.99 mA current) provided the areas that were normalized relative to the coherent and incoherent scattering peaks [15]. The normalized intensities of the machine are proportional to the concentrations used to calculate the concentrations of our samples by external calibration. The results obtained are shown in the table with a confidence interval according to Student's t-test at α=0.95.

- **Detection limit, Accuracy and sensitivity**:
  - Limitations: Elements with an atomic number lower than that of carbon cannot be analyzed by X-ray fluorescence [14]. The detection limit depends on the excitation source used and the experimental conditions under which the analysis is performed. It is around 10 ppm for elements such as (Zn, Cu, Pb) and can reach 100 ppm or even 500 ppm for light elements.
  - Accuracy varies depending on the amount of material available for analysis. It also depends on the elements being sought and the matrix in which the element is found.
  - Sensitivity depends on the sample preparation method and the material being analyzed. It varies with the chemical elements. It approaches µg/g when working without dilution on a sample of around one gram.

The analyses were performed using a XEPOS fluorescence spectrometry (EDXRF), and the results are recorded in Table 1. Table 1 shows the major and trace element contents of the analyzed samples, with histograms in Figures 17 and 18; the major and trace elements are illustrated in grams.

Table 1. *Data from the particle size analysis of the six samples*

Oxides	KS1	ND10	NG21	ZG 2	KM 1	KSK 2	Units
Na2O	0.299	0.286	0.379	0.439	0.306	0.219	%
MgO	0.1328	0.1504	0.1234	0.1621	0.4762	0.2341	%
Al2O3	8.823	11.37	10.77	16.214	8.782	7.389	%
SiO2	43.12	49.01	55.55	57.89	41.56	63.14	%
P2O5	0.2262	0.3986	0.1637	0.2133	0.1851	0.1409	%
SO3	0.03726	0.03910	0.0454	0.04871	0.02993	0.1394	%
K2O	3.073	2.538	3.58	0.02931	3.109	3.883	%
CaO	14.18	1.678	2.985	0.00478	15.49	3	%
TiO2	0.5651	1.347	0.5761	0.4302	0.4437	0.4695	%
MnO	1684	480.5	1027	72.23	2926	791.6	%
Fe2O3	3.175	5.917	3.274	1.112	3.614	2.352	%
V2O5	0.0223	0.039	0.018	0.0443	0.0148	0.0215	ppm
Cr2O3	80	176.1	65	16.54	60.9	57.5	ppm
CoO	-	78.3	-	1.89	-	-	ppm
NiO	35.9	88.0	-	17	34.3	-	ppm
CuO	30.1	14.1	28.9	32	-	20.1	ppm
ZnO	28.2	59.1	36.9	11.3	27.1	27.6	ppm
As2O3	1.08	-	4.3	0.21	21.1	<1.4	ppm
Rb2O	126.7	91.3	130.5	0.135	117.3	128.2	ppm
SrO	0.01297	0.00838	0.01526	0.00001	0.01286	0.01723	ppm
ZrO2	0.06656	0.1398	0.05013	0.00812	0.03003	0.07616	ppm
Nb2O5	16.5	37.5	15.8	1.3	11.7	11.9	ppm
SnO2	-	-	-	2.6	2.15	8.6	ppm
Sb2O5	-	21.9	10.3	-	-	14.2	ppm
Ta2O5	<1.2	-	<1.2		-	<1.2	ppm
PbO	13.7	15.9	16.9	14.2	12.2	19.9	ppm

The table of chemical analyses of sandstone (Table 1) shows that the six samples are composed of the following oxides: SiO_2, Al_2O_3, Fe_2O_3, K_2O, MgO, MnO, Na_2O, P_2O_5, SO_3, CaO, and Ti_2O. The trace elements are: tantalum (Ta), Cr (chromium), Ni (nickel), Cu (copper), Zn (zinc), As (arsenic), V (vanadium), Co (cobalt), Rb (rubidium), Sr (strontium), Zr (zirconium), Nb (niobium), Se (selenium), and Sb (antimony). The results of chemical analyses of the major elements are illustrated by a histogram (Figure 17), allowing for easy comparison between the different lithofacies analyzed. Also, for the trace elements was drawn a histogram (Figure 18).

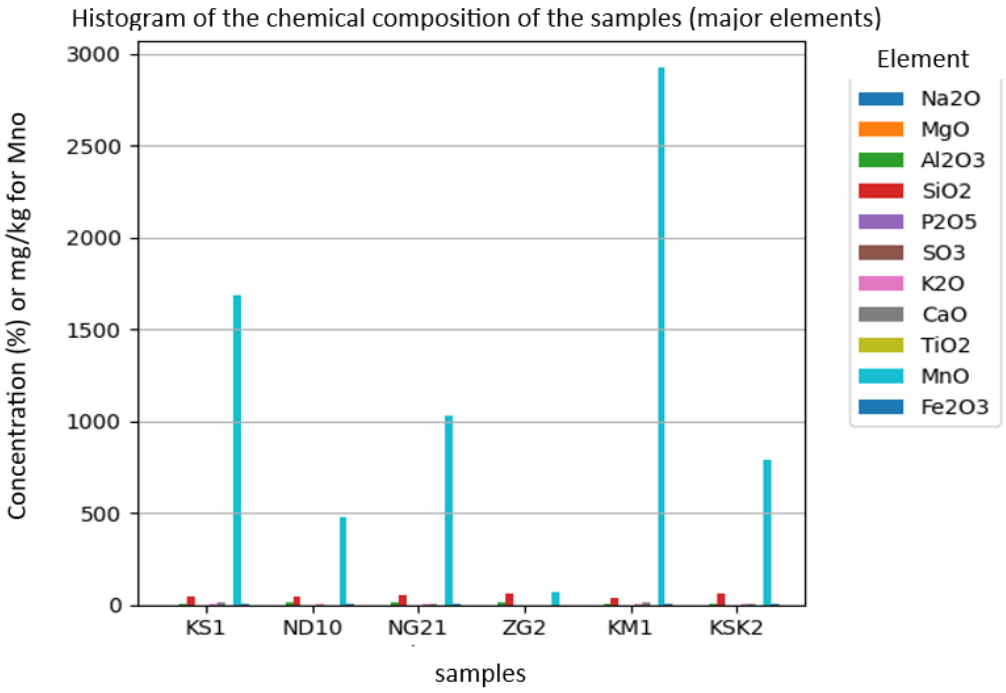

***Figure 17**. Histogram of the chemical composition of the samples for the major elements. The x-axis shows the series of samples analyzed and the y-axis shows the percentage of each element.*

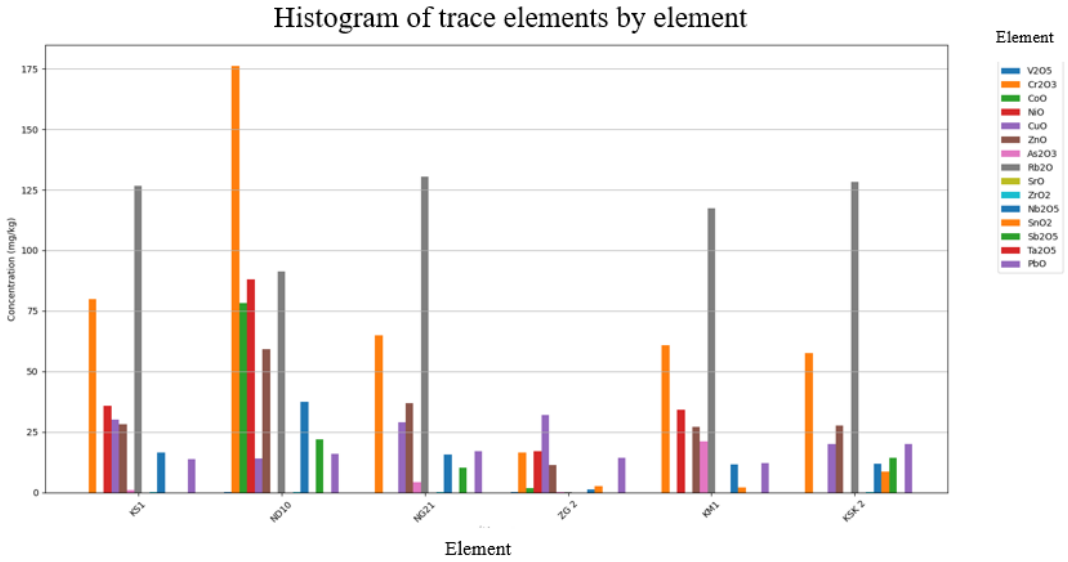

***Figure 18**. Histogram of trace elements.*

As a legend for the elements, we have, from sky blue to dark blue: alumina (Al2O3), magnesium oxide (MgO), titanium oxide (TiO2), and sodium oxide (Na2O); in orange: calcium (CaO); in light gray: iron (III) oxide, in yellow: potassium oxide (K2O), in dark gray: silicon oxide, in red: phosphate (P2O5), in green: manganese oxide, and in brown: sulfur oxide (SO3).

The histogram in Figure 17 illustrates the chemical composition of the major elements in six sediment samples (KS1, ND10, NG21, ZG2, KM1, KSK2). Overall, silica (SiO_2) dominates the content, reaching percentages above 40% in all samples, which is characteristic of siliceous sediments, often associated with a high presence of quartz. Alumina (Al_2O_3), an indicator of clays, is also present in significant quantities, especially in sample ZG2, suggesting a notable clay contribution. Manganese (MnO) has exceptionally high levels, particularly in samples KM1 and KS1, which may indicate a diagenetic influence or enrichment linked to post-sedimentary chemical processes. Calcium (CaO) and potassium (K_2O), often associated with carbonates and feldspars or micas, respectively, vary greatly, reflecting the heterogeneity of the mineralogical sources. Thus, this composition reflects the diversity of lithological inputs and geochemical conditions. Geochemical analysis of trace elements (Figure 18) present in the samples (KS1, ND10, NG21, ZG2, KM1, KSK2) reveals diversity in sedimentary sources and post-depositional processes. High concentrations of chromium, nickel, and cobalt, particularly in ND10, KS1, and NG21, indicate a significant contribution from ultramafic or basaltic rocks, probably originating from a poorly altered basic magmatic basement. At the same time, the high rubidium, niobium, and zirconium contents, especially in NG21 and ND10, suggest a significant contribution from evolved felsic rocks, such as granites or gneisses.

The KM1 and KSK2 samples stand out for their enrichment in arsenic, antimony, lead, and tin, elements often linked to hydrothermal processes or anthropogenic influences. These enrichments could indicate the proximity of metal mineralization or secondary sources rich in sulfides. Furthermore, the low strontium concentrations in all samples indicate advanced alteration or a low input of carbonates or plagioclases, while the moderate levels of vanadium suggest a moderately oxidizing deposit environment.

Overall, these results reflect the heterogeneity of sedimentary sources, combining basic and felsic inputs with localized hydrothermal or diagenetic signatures [28]. They highlight the complexity of transport, alteration, and deposition processes in the studied environment [13].

STATE OF ROCK ALTERATION

In order to elucidate the possible effects of alteration due to either metamorphism or meteoric alteration, the mobility of the elements is marked by the trace of the major elements as a function of K_2O, MgO, Na_2O, and CaO.

In order to characterize and quantitatively estimate the state of alteration of a rock, various alteration indices can be used. In this work, we used the hydrothermal alteration index (AI) based on the arithmetic equation [15],[20]:

$$AI = 100 * \frac{(K_2O + M_gO)}{(K_2O + M_gO) + (Na_2O + C_aO)}$$

This index allows hydrothermal alteration to be characterized by evaluating the mobility of K_2O, MgO, Na_2O, and CaO. The closer the index is to 100%, the higher the level of rock alteration, and vice versa.

Table 2. *Weathering index of different rock samples*

Samples	KS1	ND10	NG21	ZG2	KM1	KSK2
AI (%) hydrothermal alteration index	18.13	57.79	52.40	30.13	18.50	56.12

Our samples are distributed as follows:

- KS1, KM1: low (≈ 18%); lower values indicate a less altered state or limited or absent potassium/magnesium signatures.
- ZG2: moderate (≈ 30%) show intermediate alteration, transition; progressive enrichment in K and Mg (biotite, chlorite) at the expense of sodium/calcium phases (plagioclase, albite).
- NG21, ND10, KSK2: strong (≈ 52–58%); High AI values indicate a less altered state or residual sodium/calcium dominance.

This supports the idea that ND10 and KSK2 are located in areas of more intense fluid circulation.

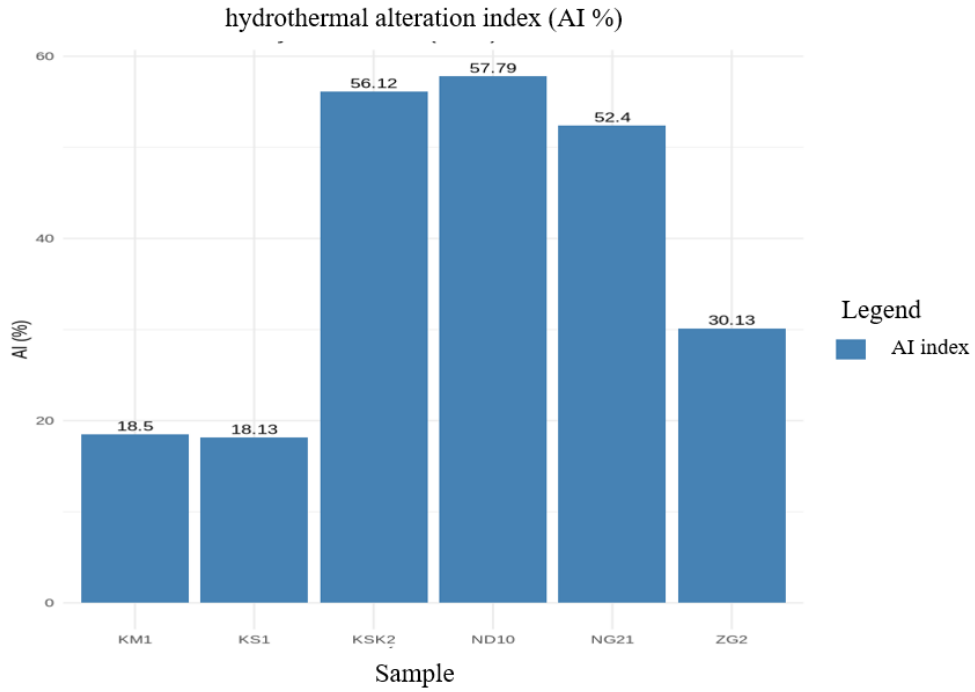

***Figure 19**. Hydrothermal alteration (HA) profile of analyzed samples.*

CONCLUSIONS

The detailed analysis of samples collected from various sites in the Inkisi region has provided important information on the lithological and geochemical composition of the geological formations. The results of petrographic and geochemical studies reveal a wide diversity of minerals, including oxides and trace elements, reflecting the geological complexity influenced by various deposition and alteration processes.

The calculated hydrothermal alteration indices show that some samples exhibit moderate to strong alteration, which may indicate more intense fluid circulation conditions in these areas. These observations underscore the importance of field data for understanding the geological dynamics and potential natural resources of the region.

The results obtained, particularly regarding porosity and permeability, suggest a favorable possibility for the presence of hydrocarbons. However, additional analyses will be necessary to establish direct correlations with the existence or absence of hydrocarbons in the Inkisi formation.

Thus, this study opens the door to future research and targeted exploration, contributing to a better understanding of the geological systems of the Inkisi region. By integrating petrographic and geochemical aspects, this research also highlights the need for a multidisciplinary approach to assess hydrocarbon potential and improve exploration strategies. This work represents a significant advance in the study of the Inkisi formation and offers promising perspectives for the exploitation of its resources.

REFERENCES

[1] Konopásek, J., Cavalcante, C., Fossen, H., Janoušek, V., 2020. Adamastor – an ocean that never existed? Earth-Science Reviews, 205, 103201.

[2] Fernandez-Alonso, M., Deblond, A., Early Neoproterozoic magmatism (1000–910 Ma) of the Central African Copperbelt and its bearing on the Rodinia reconstruction. Precambrian Research, 110(1–4), 277–306. 2001

[3] Kipata, M.L., Delvaux, D., Sebagenzi, M.N., Cailteux, J., Sintubin, M., Brittle tectonic and stress field evolution in the Pan-African Lufilian arc and its foreland (Katanga, DRC): from orogenic compression to extensional collapse, transpressional inversion and transition to rifting. Geologica Belgica, 16, 1-18. 2013.

[4] Lepersonne, J., Carte géologique et notes explicatives de la République du Zaïre. Bruxelles : Musée Royal de l'Afrique Centrale, 63 pp., 1974

[5] Delvaux, D., Kervyn, F., Macheyeki, A.S., Temu, E.B., Geodynamic significance of the TRM segment in the East African Rift (W-Tanzania): Active tectonics and paleostress in the Ufipa plateau and Rukwa basin. Journal of Structural Geology, 37, 161-180. 2012

[6] Cahen, L., Lepersonne, J., Synthèse de la géologie du Zaïre. Bruxelles, Musée Royal de l'Afrique Centrale, 495 p., 1976

[7] Tack, L., Wingate, M.T.D., Liégeois, J.-P., Fernandez-Alonso, M. and Deblond, A., Early Neoproterozoic magmatism (1000–910 Ma) of the Zadinian and Mayumbian Groups (Bas-Congo): onset of Rodinia rifting at the western edge of the Congo craton. Precambrian research, 110, 277-306, 2001.

[8] Alvarez, P., Maurin, J.-C., Vicat, J.-P., La formation de l'Inkisi (Supergroupe ouest-congolien) en Afrique centrale (Congo et Bas-Zaïre): un delta d'âge Paléozoïque comblant un bassin en extension. Journal of African Earth Sciences, 20, 119-131, 1995

[9] Delvaux, D., Ganza, G., Mees, F., Lahogue, P., The use of hybrid fractures in paleostress determinations: test case with the the Palygorskite-bearing fractures in the Kinshasa area, DR Congo, Geophysical Research Abstracts, Vol. 16, EGU2014-8917, 2014

[10] Boudzoumou, F., Etude sédimentologique de la Formation d'Inkisi dans la région de Brazzaville. Thèse de Doctorat, Université Marien Ngouabi. 1986

[11] Cayeux, L., Introduction à l'étude pétrographique des roches sédimentaires. Imprimerie Nationale. 1916

[12] Harding, T.P., Lowell, J.D., Structural styles, their plate tectonic habitats and hydrocarbon traps in petroleum provinces. Bull. Am. Ass. Petrol. Geol., 83, 1-24. 1979.

[13] Guilbert, J.M., Park, C.F., The Geology of Ore Deposits. W. H. Freeman. 1986

[14] Pirajno, F., Hydrothermal Processes and Ore Systems. Springer. 2009

[15] Barnes, H.L., Geochemistry of Hydrothermal Ore Deposits. John Wiley & Sons. 1997

[16] Gaboury, D., Paramètres des altérations hydrothermales des gisements de type VMS et aurifères. CONSOREM. 2004

[17] Mathieu, L., Quantifier l'altération hydrothermale: l'apport des calculs normatifs. CONSOREM. 2015

[18] Affaton, P., Kalsbeek, F., Boudzoumou, F., Trompette, R., Thrane, K., Frei, R., The Pan-African West Congo belt in the Republic of Congo (Congo Brazzavile): Stratigraphy. of the Mayombe and West Congo. Precambrian Research, 272, 185-202, 2016.

[19] Kadima, E., Delvaux, D., Sebagenzi, S.N., Tack, L., Kabeya, S.M., Structure and geological history of the Congo Basin: an integrated interpretation of gravity, magnetic and reflection seismic data. Basin Research, 23, 499-527, 2011.

[20] Ishikawa, Y., Sawaguchi, T., Iwaya, S., Horiuchi, M., Délimitation des cibles de prospection des gisements de Kuroko d'après les modes de volcanisme de la dacite sous-jacente et les halos d'altération. Mining Geology, 26, 105-117, 1976

[21] MacKenzie W.S., Adams A.E., Brodie K.H., Rocks and Minerals in Thin Section: A Color Atlas, 2nd edition, Taylor & Francis Group, London, 2017

[22] Beaux J.F., Platevoet B., Fogelgesang J.F., Atlas de pétrologie, 1st edition, Dunod, Paris, 2012

[23] Nkodia, H.M.D.-V., Style structurale et tectonique de la formation de l'Inkisi. MSc Thesis. Brazzaville, Marien Ngouabi, 93 pp., 2017.

[24] Biju-Duval B., Géologie sédimentaire, Ed. Technip, Paris, 72 pp., 1999

[25] Dadet, P., Géologie du bassin de la Cuvette Congolaise. BRGM, 1969

[26] Monza, M.A., Lohadje, J.E., Keto, F.T., Jibikila, R.M., Tshiani, N.B., Contribution of seismic and geothermal data analysis to the assessment of the hydrocarbon potential of the central basin of the DR Congo, Romanian Journal of Petroleum & Gas Technology, 5(1), 95-110, 2024

[27] Boggs, S., Principles of Sedimentology and Stratigraphy. Pearson Prentice Hall. 2006

[28] Bathurst, R.G.C., Carbonate Sediments and Their Diagenesis. Elsevier. 1975

Received: September 2025; Revised: October 2025; Accepted: November 2025; Published: November 2025